
Figures and figure supplements

Latrophilin-2 and latrophilin-3 are redundantly essential for parallel-fiber synapse function in cerebellum

Roger Shen Zhang *et al*

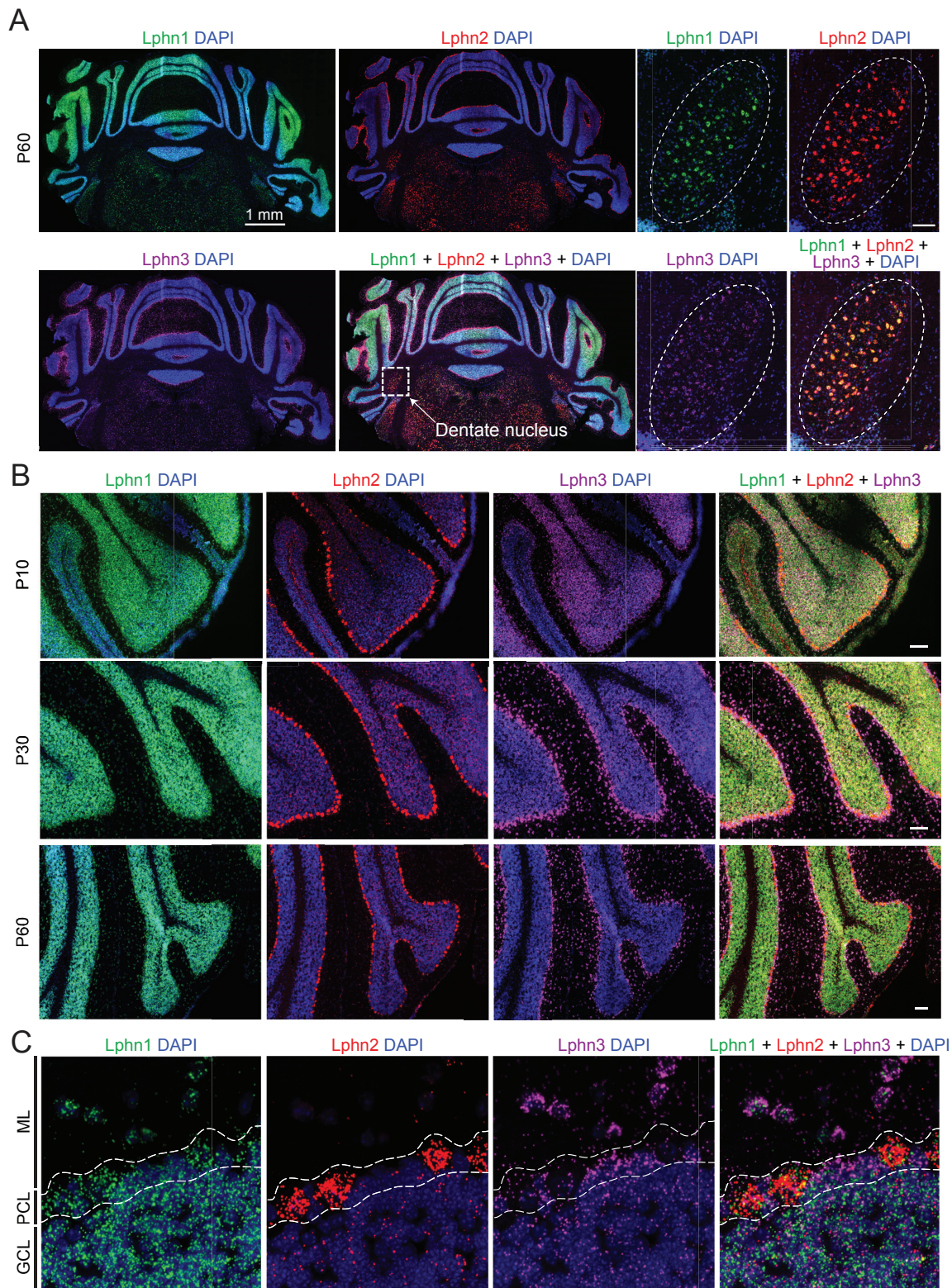


Figure 1. Differential expression of Lphn1, Lphn2, and Lphn3 mRNAs in cerebellum. (A) Overview of the expression of latrophilins in the cerebellum. smRNA-FISH was performed on mouse cerebellar sections at P60 with probes against Lphn1 (green), Lphn2 (red) and Lphn3 (purple) to visualize Figure 1 continued on next page

Figure 1 continued

expression of latrophilin transcripts (left, overview of whole cerebellum; right, expanded images of the dentate nucleus, scale bar: 100 μ m). (B) Time course of latrophilin expression in cerebellar cortex. smRNA-FISH for all three latrophilin isoforms was performed with mouse cerebellar sections at P10, P30 and P60 (scale bars: 100 μ m). (C) Expanded view of the cerebellar cortex at P60 showing expression of latrophilin transcripts in the molecular layer (ML), Purkinje cell layer (PCL) and granule cell layer (GCL). Lphn1 and Lphn3 transcripts are detected in all three cerebellar layers shown, while Lphn2 transcripts are primarily identified in the Purkinje cell layer.

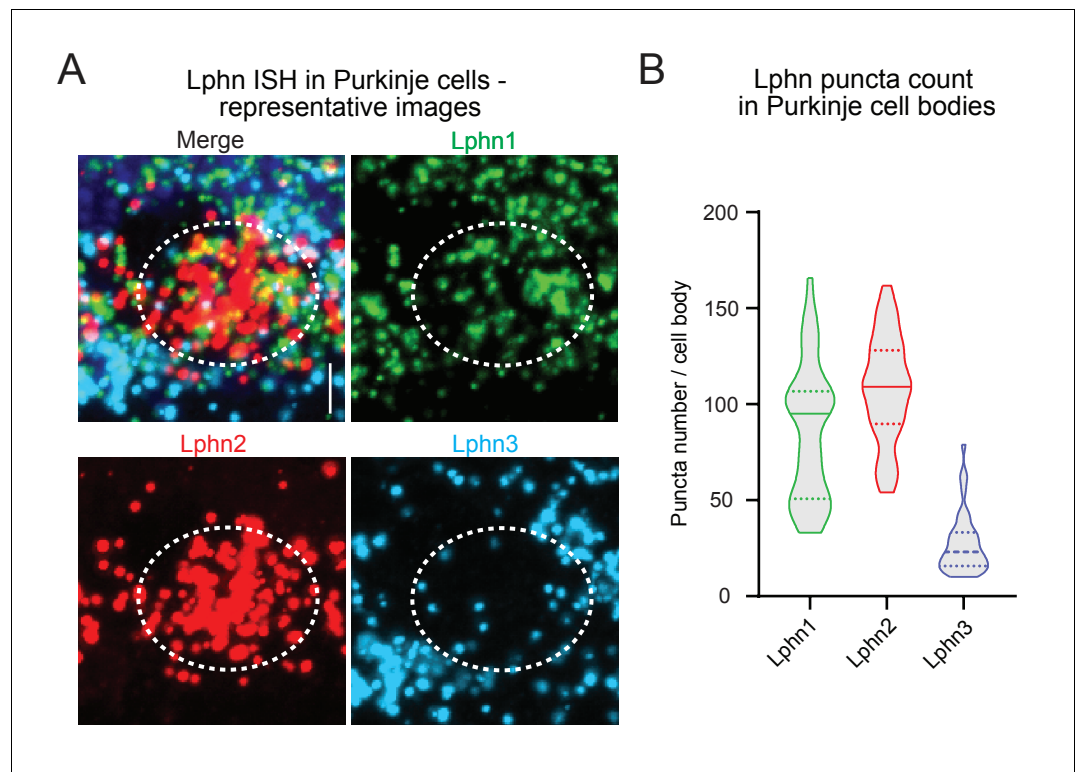


Figure 1—figure supplement 1. Lphn1 and Lphn2 transcripts are more abundant in Purkinje cell bodies than Lphn3 transcripts. (A) Expanded view of a Purkinje cell body showing transcripts of Lphn1 (green), Lphn2 (red) and Lphn3 (blue) visualized by smRNA-FISH at P30 (white circle: Purkinje cell body, scale bar: 5 μ m). (B) Lphn1 and Lphn2 transcripts are more abundant than Lphn3 transcripts in Purkinje cells. The number of Lphn puncta per Purkinje cell body were manually counted (n = 42 cells from one mouse; solid line: median; dashed lines: interquartile range).

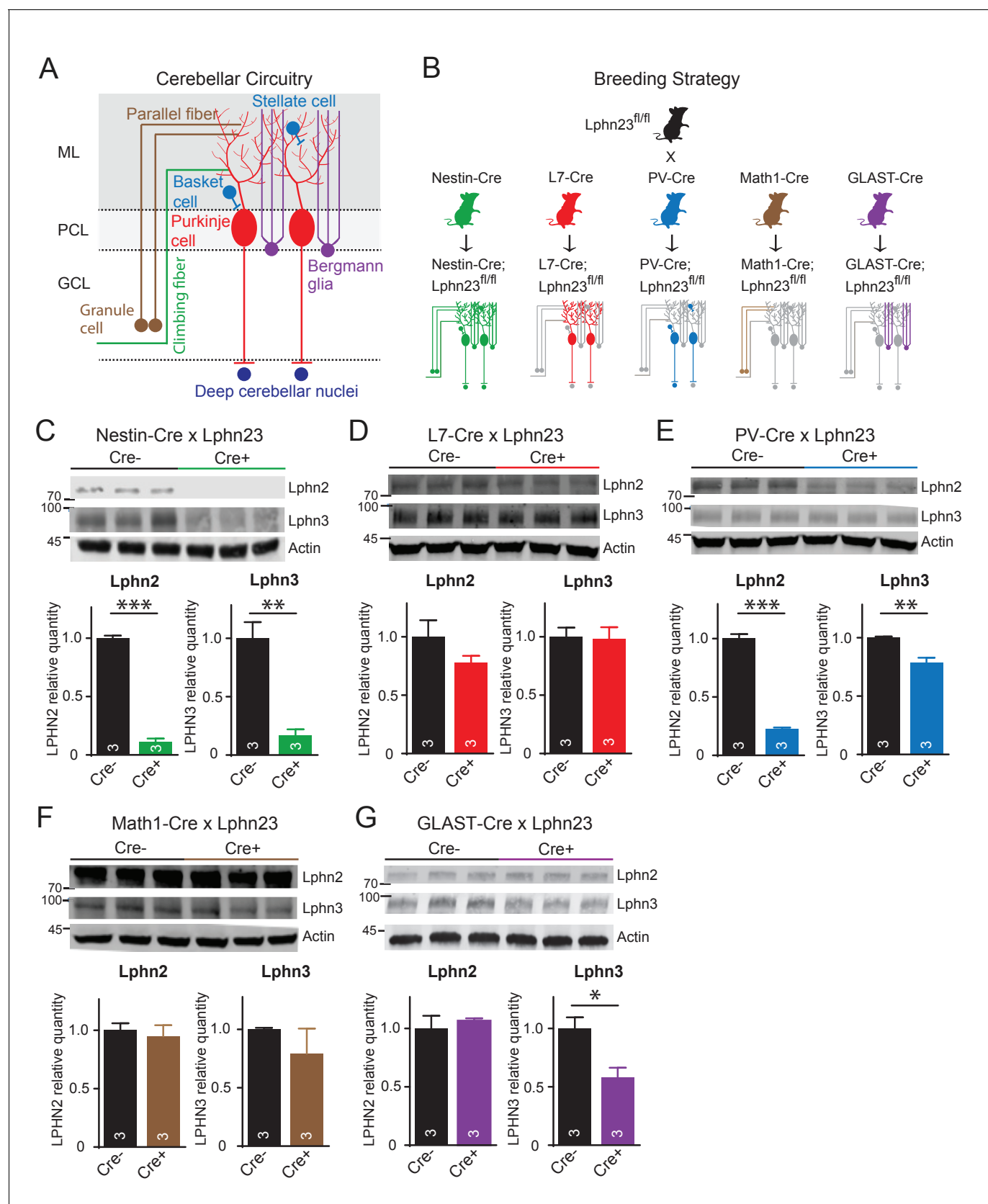


Figure 2. Cell type-specific deletion of Lphn2 and Lphn3 induce differential reduction in Lphn2 and Lphn3 protein levels. (A) Schematic of the cellular circuitry of the cerebellar cortex. Shown are parallel-fiber (brown) and climbing-fiber (green) excitatory inputs onto Purkinje cells, basket and stellate cells. (B) Breeding strategy. (C-G) Western blots and bar graphs showing LPHN2 and LPHN3 relative quantities in different cell types. Figure 2 continued on next page

Figure 2 continued

inhibitory interneurons (blue-green) in the molecular layer, Bergmann glia (purple) extending processes into the molecular layer and Purkinje cell outputs onto deep cerebellar nuclei (dark blue). **(B)** Breeding strategy for generation of cell type-specific knockouts of Lphn2 and Lphn3 using various transgenic Cre-driver mouse lines. The specific cell types targeted by the Cre lines are as follows: Nestin-Cre: all neurons and glia, L7-Cre: Purkinje cells, PV-Cre: molecular layer interneurons (basket and stellate cells), Purkinje cells and some deep cerebellar nuclei neurons, Math1-Cre: granule cells, GLAST-Cre: Bergmann glia. **(C–G)** Conditional knock-in mice with mVenus-tagged Lphn2 and HA-tagged Lphn3 were crossed with transgenic Cre-driver lines to examine the cell type-specific expression of Lphn2 and Lphn3 by immunoblotting in cerebellum of littermate mice with and without Cre recombinase expression (top, representative immunoblot images; bottom, summary graphs). **(C)** Expression of Lphn2 and Lphn3 in cerebellum is largely abolished in nestin-Cre positive mice, indicating that both are predominantly expressed in neurons and glia. **(D)** Lphn2 and Lphn3 expression in Purkinje cells is limited compared to their total cerebellar expression, although this may be confounded by the relative scarcity of Purkinje cells relative to other cell types in cerebellum. **(E)** Lphn2 (~80%) and Lphn3 (~20%) expression in PV-positive neurons make up a significant proportion of total Lphn cerebellar expression. **(F)** Lphn2 and Lphn3 expression in granule cells is limited relative to total cerebellar Lphn expression. **(G)** A significant proportion of Lphn3 (~50%) but not of Lphn2 in cerebellum is expressed in Bergmann glia, a cerebellar type of astrocyte. All numerical data are means \pm SEM; numbers in bars represent number of mice tested. Statistical analyses were performed using Student's t-test (* $p < 0.05$; ** $p < 0.01$; *** $p < 0.001$).

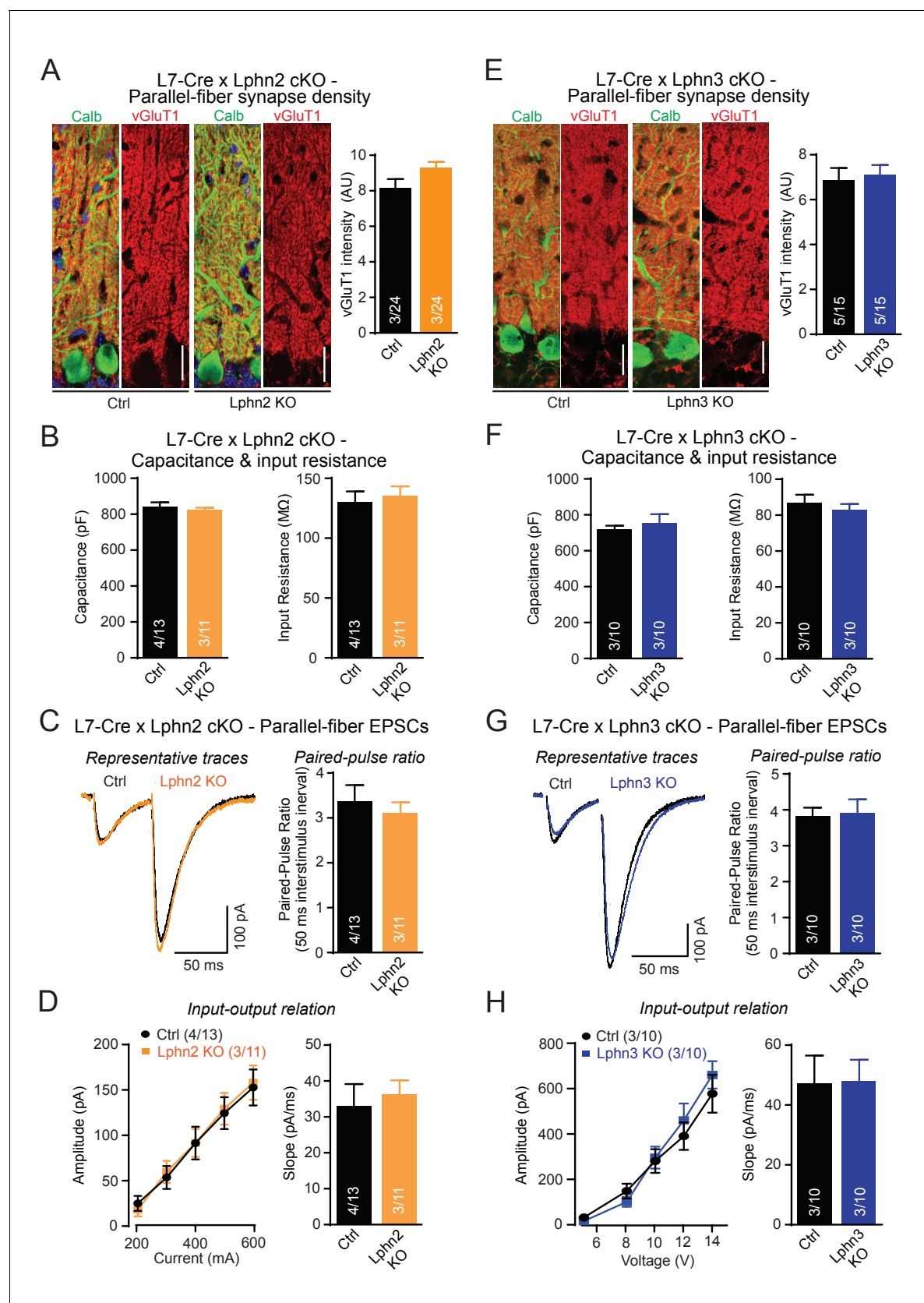


Figure 3. Individual deletions of Lphn2 or Lphn3 in Purkinje cells do not detectably affect parallel-fiber synapse density or function. (A) Lphn2 deletion from Purkinje cells does not affect parallel-fiber synapse staining as shown by unchanged vGluT1 staining intensity. vGluT1 specifically labels parallel-fiber synapses. Figure 3 continued on next page

Figure 3 continued

fiber synapses and vGluT1 staining intensity serves as a proxy for parallel-fiber synapse density (left, representative images with vGluT1 in red and calbindin in green; right, summary graph). **(B)** Purkinje cell capacitance (left) and input resistance (right) are unchanged by Lphn2 KO. **(C–D)** Lphn2 deletion does not affect evoked parallel-fiber synaptic transmission measured by recording parallel-fiber excitatory postsynaptic currents (parallel-fiber EPSCs) from Purkinje cells evoked by electrical stimulation in the upper molecular layer. The paired-pulse ratio (PPR, **(C)**), input-output relation and EPSC slope **(D)** are unchanged by Lphn2 deletion (C left, representative traces with 50 ms inter-stimulus interval; C right, summary graph of PPR; D, summary graphs of input-output relation and EPSC slope). **(E)** Lphn3 KO does not affect parallel-fiber synapse density (as in A). **(F)** Purkinje cell capacitance (left) and input resistance (right) are unchanged by Lphn3 KO. **(G–H)** Same as **(C–D)** but for the Lphn3 KO, demonstrating that the Lphn3 deletion from Purkinje cells also does not affect parallel-fiber synaptic transmission. All scale bars are 20 μm . Numerical data are means \pm SEM; numbers in bars represent independent experiments/number of cells tested.

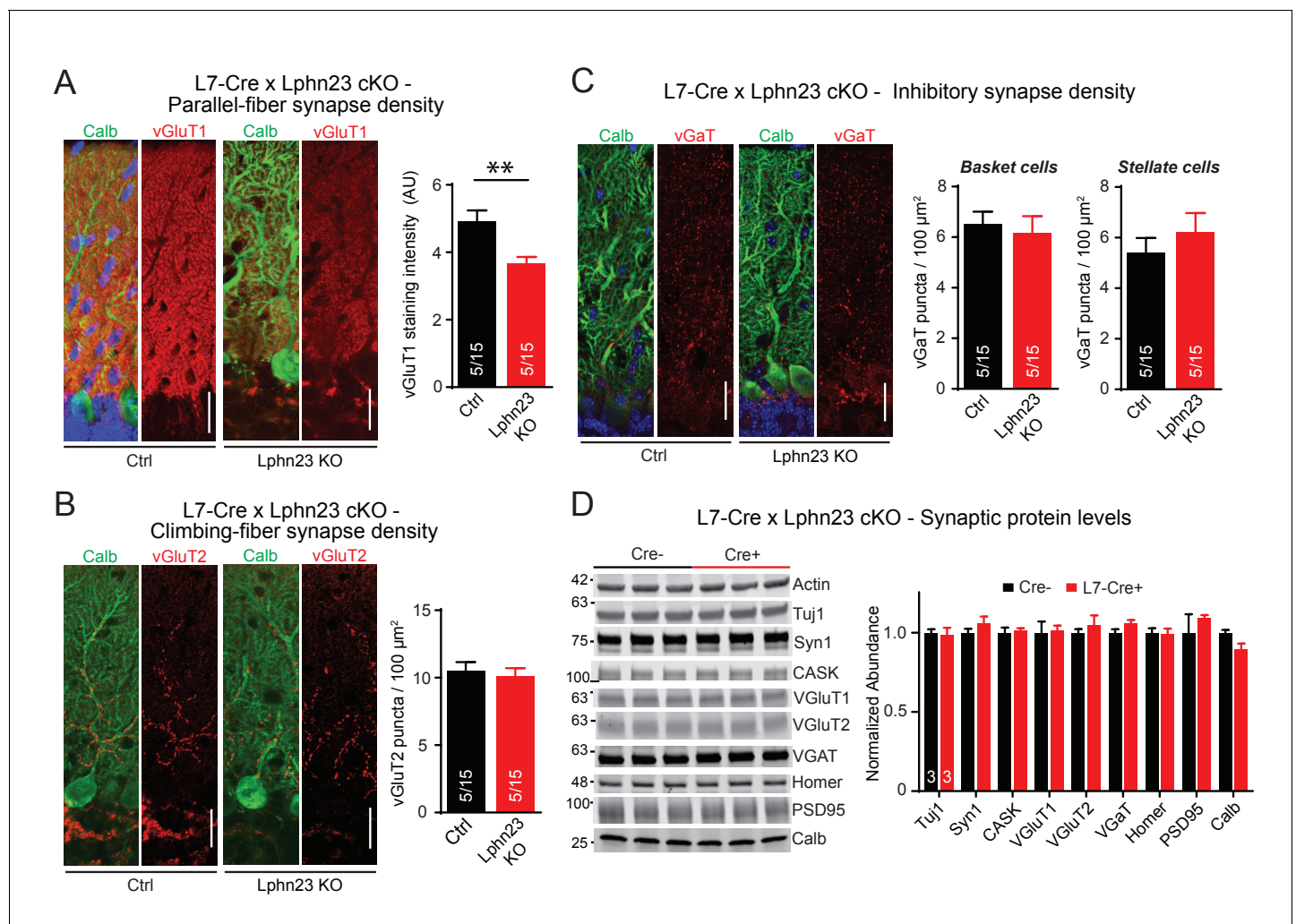


Figure 4. Double deletion of Lphn2 and Lphn3 in Purkinje cells decreases parallel-fiber synapse density but has no effect on climbing-fiber synapse density, inhibitory synapse density in the cerebellar cortex or synaptic protein composition of the cerebellum. (A) Deletion of both Lphn2 and Lphn3 from Purkinje cells reduces parallel-fiber synapse staining as shown by reduced vGluT1 staining intensity that specifically labels parallel-fiber synapses and has been previously shown to be a proxy for parallel-fiber synapse density (left, representative images of vGluT1 in red and calbindin in green; right, summary graph). (B) The Lphn2/3 double deletion from Purkinje cells does not alter climbing-fiber synapse density as visualized by vGluT2 puncta staining. Climbing-fiber synapse density was quantified by counting vGluT2 puncta (red) co-stained with calbindin (green) as a function of Purkinje cell dendrite area (left, representative images; right, summary graph). (C) The Lphn2/3 double deletion from Purkinje cells does not alter inhibitory basket-cell or stellate-cell synapse density as shown by vGAT puncta staining. Basket-cell synapse density was quantified by measuring vGAT puncta density (red) on Purkinje cell bodies identified by calbindin staining (green), while stellate-cell synapse density was quantified by measuring vGAT puncta density in the upper half of the molecular layer (left, representative images; right, summary graph). (D) The Lphn2/3 double deletion from Purkinje cells does not alter synaptic protein levels from whole cerebellum (top, representative immunoblots; bottom, summary graph of protein abundance normalized to actin loading controls, $n = 3$ each). All scale bars are 20 μm . Data are represented as means \pm SEM; numbers in bars in A, B, C represent independent experiments/number of sections imaged. ** $p < 0.01$ (two-tailed t test).

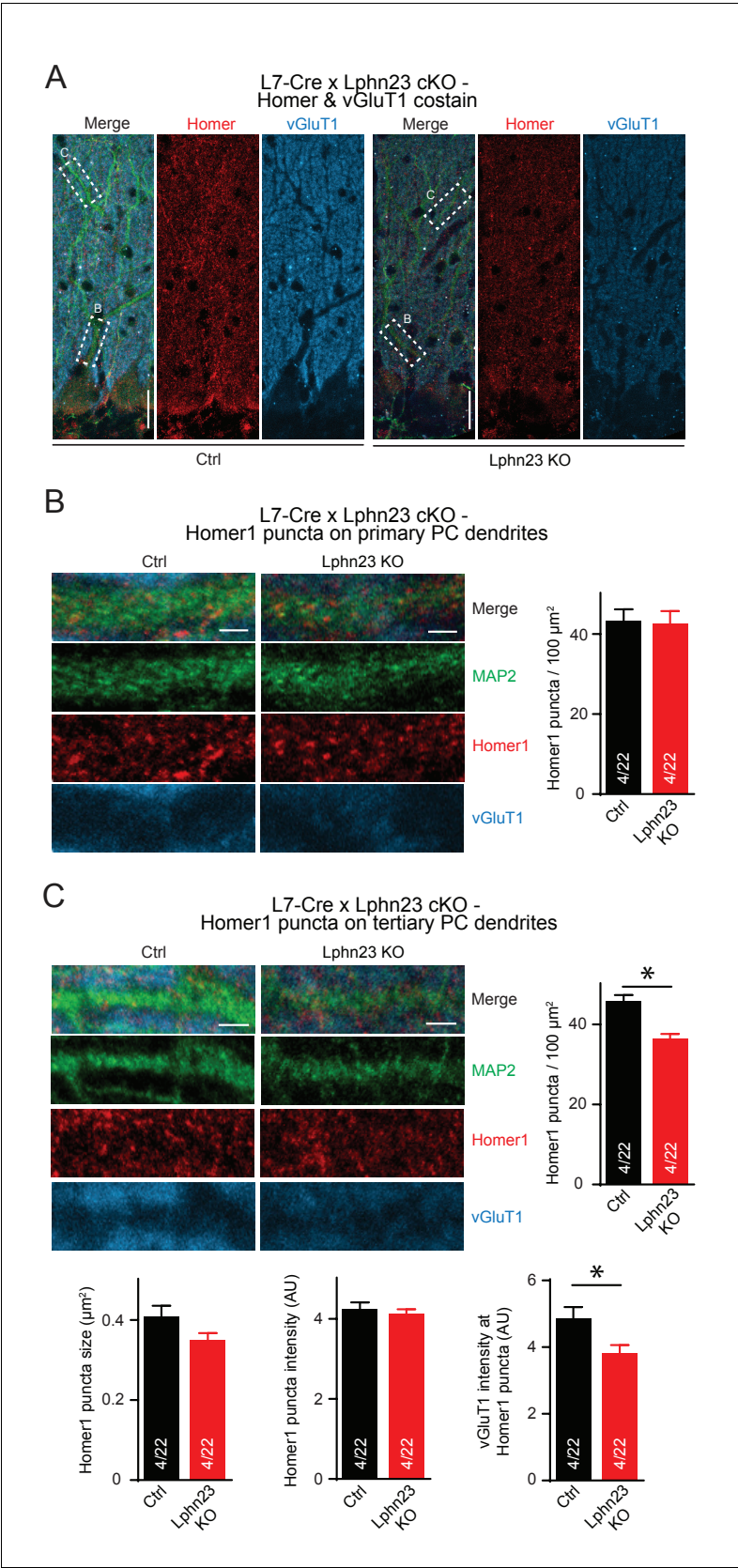


Figure 4—figure supplement 1 continued

Purkinje cells does not affect Homer1 puncta density on primary Purkinje cell dendrites but reduces Homer1 puncta density on tertiary dendrites from the distal half of the cerebellar cortex. Climbing-fiber inputs synapses onto primary Purkinje cell dendrites while parallel-fiber inputs synapse onto tertiary dendrites. (A), representative images of Homer1 (red) co-stained with vGluT1 (blue) and MAP2 (green). (B) Homer1 puncta density on primary Purkinje cell dendrites is unchanged (left: representative images; right: summary graph). (C) Homer1 puncta density and vGluT1 staining intensity at Homer1 puncta is reduced by Lphn2/3 double-deletion at tertiary Purkinje cell dendrites but Homer1 puncta size and staining intensity is unchanged (top left: representative images; top right and bottom: summary graphs). Scale bars are 20 μm in A and 2 μm in B-C. Data are means \pm SEM; numbers in bars represent independent experiments/number of cells tested. * $p < 0.05$ (two-tailed t test).

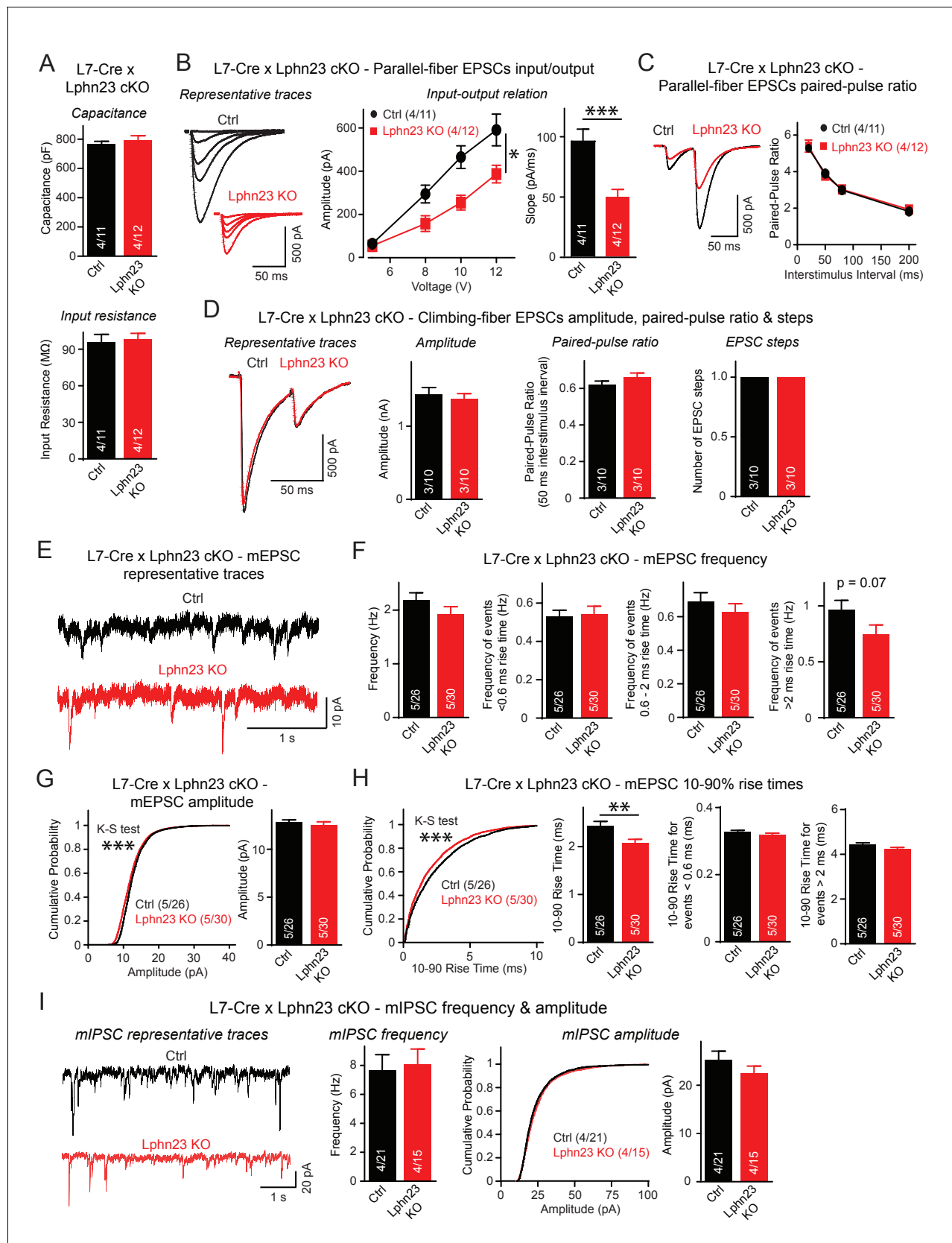


Figure 5. Double deletion of Lphn2 and Lphn3 from Purkinje cells suppresses parallel-fiber synaptic transmission without altering climbing-fiber synaptic transmission. (A) The Lphn2/3 double deletion from Purkinje cells does not affect their capacitance or input resistance. (B) The Lphn2/3 double deletion from Purkinje cells suppresses parallel-fiber EPSCs input/output relation. (C) The Lphn2/3 double deletion from Purkinje cells suppresses parallel-fiber EPSCs paired-pulse ratio. (D) The Lphn2/3 double deletion from Purkinje cells does not affect climbing-fiber EPSCs amplitude, paired-pulse ratio & steps. (E) Representative traces of mEPSCs in L7-Cre x Lphn23 cKO mice. (F) mEPSC frequency in L7-Cre x Lphn23 cKO mice. (G) mEPSC amplitude in L7-Cre x Lphn23 cKO mice. (H) mEPSC 10-90% rise times in L7-Cre x Lphn23 cKO mice. (I) mIPSC frequency & amplitude in L7-Cre x Lphn23 cKO mice. Figure 5 continued on next page

Figure 5 continued

deletion from Purkinje cells impairs parallel-fiber synaptic transmission as shown by diminished input-output relation and reduced slope of parallel-fiber excitatory postsynaptic currents (EPSCs) recorded from Purkinje cells (left, representative traces showing parallel-fiber EPSCs at increasing stimulus intensities; right, summary graph of input-output relation and parallel-fiber EPSC slope). (C) The *Lphn2/3* double deletion from Purkinje cells has no effect of the paired-pulse ratio (PPR) of parallel-fiber EPSCs (left, representative traces of parallel-fiber-EPSCs of identical stimulus intensity with a 50 ms inter-stimulus interval; right, summary graph of PPRs with varying inter-stimulus intervals). (D) The *Lphn2/3* double deletion from Purkinje cells does not affect climbing-fiber synaptic transmission or pruning with no differences observed in climbing-fiber EPSC amplitude, PPR or the number of steps in the evoked climbing-fiber response (left, representative traces of climbing-fiber EPSCs with a 50 ms inter-stimulus interval; right, summary graphs of climbing-fiber EPSC amplitude, PPR and number of steps). (E–F) The *Lphn2/3* double deletion from Purkinje cells does not alter the frequency of spontaneous miniature excitatory postsynaptic currents (mEPSCs) but reduces the frequency of mEPSCs with rise times greater than 2 ms (E, representative traces of mEPSCs; F, summary graphs of mEPSC frequency of all events and events separated by 10–90% rise times). A majority of mEPSCs with 10–90% rise times under 0.6 ms are derived from climbing-fibers which synapse onto proximal Purkinje cell dendrites, while a majority mEPSCs with 10–90% rise times greater than 2 ms arise from parallel-fibers which synapse onto distal Purkinje cell dendrites. A trend nearing significance was observed for lower frequency of mEPSCs with 10–90% rise times greater than 2 ms in *Lphn2/3* double KO cells compared to control ($p=0.07$). (G) The *Lphn2/3* double deletion from Purkinje cells has minimal effects on mEPSC amplitude (left, cumulative frequency relation of mEPSC amplitudes; right, summary graph). A significant difference in the cumulative frequency relation of mEPSC amplitudes was observed between *Lphn2/3* double KO and control by the Kolmogorov–Smirnov test but no significant difference in average mEPSC amplitude was identified by a two-tailed t test. (H) The *Lphn2/3* double deletion from Purkinje cells reduces the 10–90% rise time of mEPSCs (left, cumulative frequency relation of rise times; right, summary graphs of all rise times, rise times less than 0.6 ms and rise times greater than 2 ms). Both the average and cumulative frequency relation of 10–90% rise times were significantly different between *Lphn2/3* double KO and control, but no difference in average 10–90% rise times was detected in the subsets of mEPSCs with rise times under 0.6 ms or greater than 2 ms. (I) The *Lphn2/3* double deletion from Purkinje cells does not affect amplitude or frequency of spontaneous miniature inhibitory post-synaptic currents (mIPSCs) recorded from Purkinje cells (left, representative traces of mIPSCs; middle, summary graph of mIPSC frequency; right, cumulative frequency plot and summary graph of mIPSC amplitudes). Data are means \pm SEM; numbers in bars represent independent experiments/number of cells tested. * $p<0.05$, ** $p<0.01$, *** $p<0.001$ (two-tailed t test and two-way ANOVA).

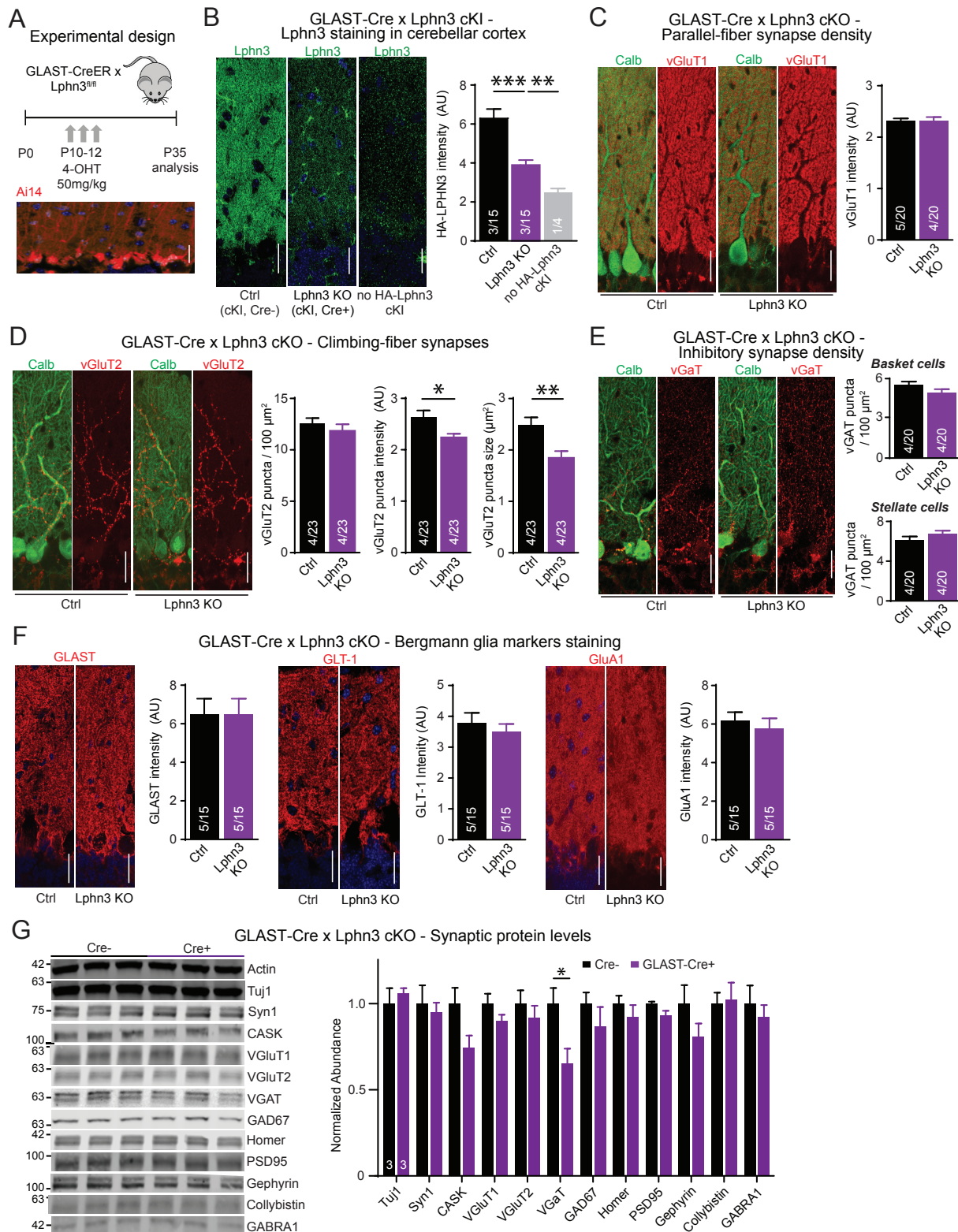


Figure 6. Deletion of Lphn3 in Bergmann glia has minimal effects on parallel-fiber, climbing-fiber or inhibitory synapse staining in the cerebellar cortex, Bergmann glia staining intensity, or synaptic protein composition of the cerebellum. (A) Schematic of experimental procedure. Lphn3 cKO mice were Figure 6 continued on next page

Figure 6 continued

crossed to the GLAST-CreER line to allow for tamoxifen-inducible Cre recombinase expression in glia. Mice were injected with 50 mg/kg of 4-hydroxytamoxifen (4-OHT) once daily from P10-12 and analysis was performed at P35. Bottom image shows a cerebellar section from a GLAST-CreER mouse with an Ai14 (Cre-dependent tdTomato) allele treated with the same induction protocol, demonstrating widespread Cre expression in Bergmann glia. (B) Lphn3 deletion from Bergmann glia reduces the intensity of HA-Lphn3 staining in the molecular layer of cerebellar sections (left, representative images; right, summary graph). Because of significant background staining in wild-type sections, the analysis shown compares staining for HA of HA-Lphn3 knock-in sections lacking Cre with those of the HA-Lphn3 knock-in with Bergmann glia deletion and of a control lacking the HA-Lphn3 knock-in allele. (C–E) Lphn3 deletion from Bergmann glia does not change parallel-fiber (C), climbing-fiber (D) or molecular-layer interneuron (E) synapse density in cerebellar cortex as visualized by vGluT1, vGluT2 and vGAT staining, respectively. Sections were double labeled for vGluT1, vGluT2, or vGAT (red) and calbindin (green, to label Purkinje cells). In (E) a significant decrease in vGluT2 puncta intensity and size was observed. (F) Lphn3 deletion from Bergmann glia does not alter the levels and distribution of three Bergmann glial marker proteins important for glial function, GLAST, GLT-1 and GluA1 (red). (G) Deletion of Lphn3 from cerebellar Bergmann glia has little effect on the synaptic protein composition of the cerebellum (left, representative immunoblots of a panel of synaptic proteins in cerebellar lysates; right, summary graph of normalized synaptic protein abundance, $n = 3$ each). Expression levels were normalized first to actin then to Cre negative controls. For all panels (C to F), representative images are shown on the left and summary graphs on the right. All scale bars are 20 μm . Data are means \pm SEM; numbers in bars represent independent experiments/number of sections imaged. * $p < 0.05$, ** $p < 0.01$, *** $p < 0.001$ (one-way ANOVA and two-tailed t test).

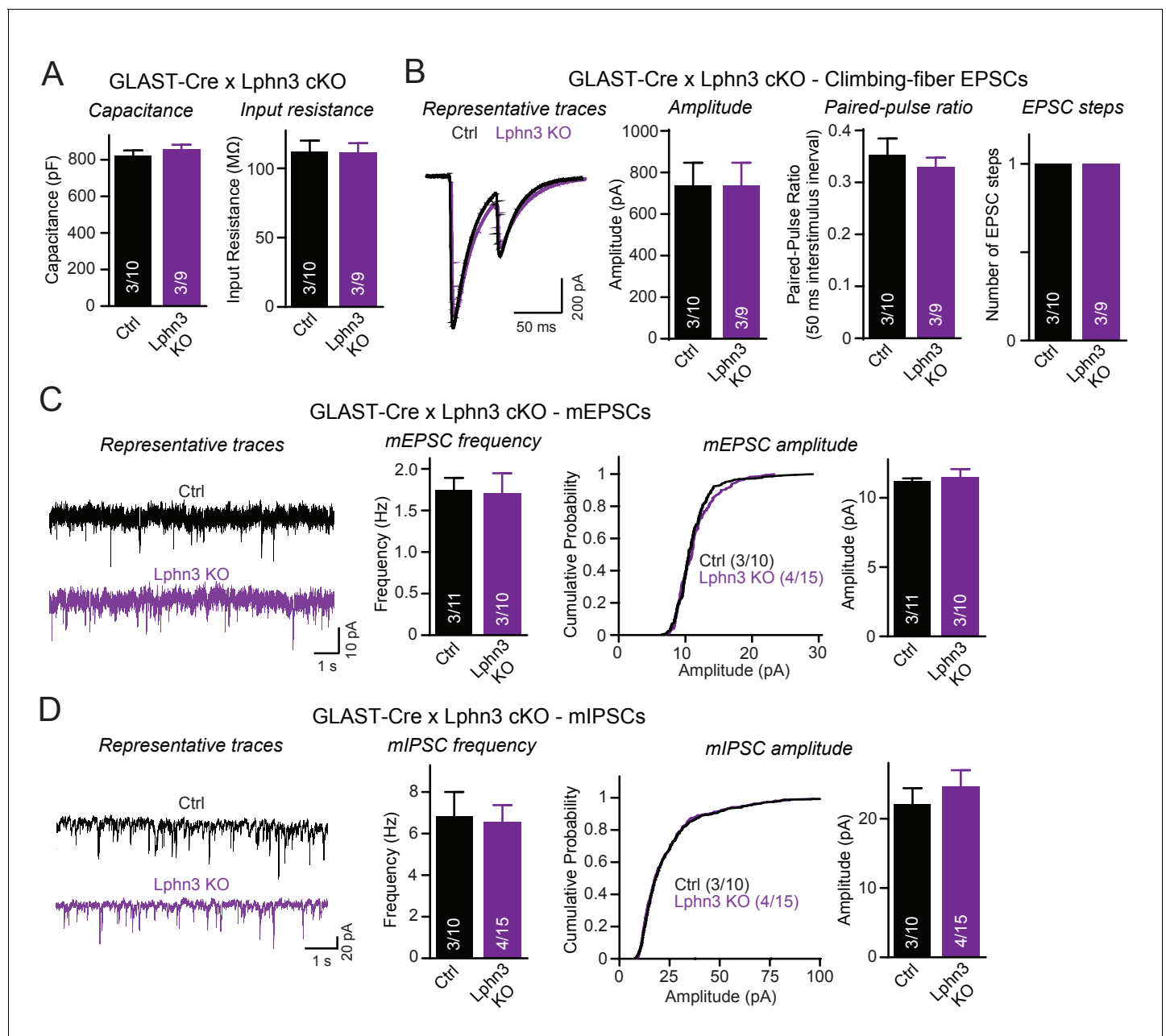


Figure 7. Deletion of Lphn3 in Bergmann glia does not alter climbing-fiber synaptic transmission or spontaneous Purkinje cell miniature currents. (A) Deletion of Lphn3 from Bergmann glia does not affect the Purkinje cell capacitance or input resistance. (B) Climbing-fiber synaptic transmission is unchanged by the deletion of Lphn3 from Bergmann glia, with no difference in climbing-fiber EPSC amplitude, paired-pulse ratio or number of steps in the EPSC response observed (left, representative traces of climbing-fiber EPSCs with a 50 ms inter-stimulus interval; right, summary graphs of climbing-fiber EPSC amplitude, PPR and number of steps). (C) Lphn3 deletion from Bergmann glia has no effect on the amplitude and frequency of spontaneous mEPSCs recorded from Purkinje cells (left, representative traces of mEPSCs; middle, summary graph of mEPSC frequencies; right, cumulative frequency plot and summary graph of mEPSC amplitudes). (D) Lphn3 deletion from Bergmann glia has no effect on the amplitude and frequency of spontaneous mIPSCs recorded from Purkinje cells (left, representative traces of mIPSCs; middle, summary graph of mIPSC frequencies; right, cumulative frequency plot and summary graph of mIPSC amplitudes). Data are means \pm SEM; numbers in bars represent independent experiments/number of cells tested.